Electron capture into the 3s and 4s states of atomic hydrogen by H^+ and D^+ impact on Ar, He, and Kr†

H. R. Dawson and D. H. Loyd
Department of Physics, Angelo State University, San Angelo, Texas 76901
(Received 24 July 1973)

Cross sections have been determined for electron capture into the 3s and 4s states of atomic hydrogen by proton and deuteron (1.2–8.2 keV) impact on Ar, He, and Kr. The He cross sections both show an exponential increase with energy. Previous structure is confirmed and additional structure is indicated in the 3s cross section for impact on Ar. These data represent the first measurements of the 3s and 4s cross sections for impact on krypton.

INTRODUCTION

Nonsymmetrical charge-transfer collisions between ions and atoms have been extensively investigated both theoretically and experimentally.[1-12] The adiabatic criterion proposed by Massey predicts that the variation of the charge-exchange cross section with velocity will show a maximum and then decrease with velocity. Although much data seem to confirm[6,12] the adiabatic criterion, some cases have been reported which indicate failure of this criterion.[1,2,9] In particular, oscillatory behavior of the cross section below the maximum has been observed. The present experiment was undertaken to examine the region below the predicted maximum in the cross section for electron capture into the 3s and 4s states of H by fast-proton impact on He, Ar, and Kr.

Cross-section measurements for electron capture into the 3s state and 4s state of H by fast-proton impact on He and Ar have been reported[1,2] at energies of 5 keV and above. This paper reports cross-section measurements for electron capture into the 3s state and 4s state of H owing to proton and deuteron impact on He, Ar, and Kr at energies less than 8.2 keV.

The techniques used for the measurement of the 3s and 4s cross sections were the same as those described in Refs. 1 and 2 and can be summarized as follows. A monoenergetic beam of protons (or deuterons) was passed through the target gas in a differentially pumped collision chamber. Charge-exchange collisions inside the chamber produced various states of atomic hydrogen in the partially neutralized beam. The beam passed from the collision chamber into an evacuated observation chamber where light emission due to the decay of excited atomic hydrogen in the beam was observed.

Cross sections for capture into the 3s state were determined by measuring the intensity of the radiation in the $3s \rightarrow 2p$ transition. Separation of the radiation due to the $3s \rightarrow 2p$ transition from radiation due to other transitions included in H_α ($n = 3 \rightarrow 2$) radiation was accomplished by measuring the H_α radiation at a point sufficiently far from the collision chamber to ensure that the short-lived 3p and 3d states had decayed to the extent that they contributed essentially no radiation.

The cross section for capture into the 4s state was determined from the measured intensity of the $4s \rightarrow 2p$ transition using the same technique to separate the $4s \rightarrow 2p$ radiation from the other H_β ($n = 4 \rightarrow 2$) radiations.

APPARATUS

A schematic diagram of the apparatus as viewed from above is shown in Fig. 1. A proton (or deuteron) beam was extracted from an Ortec model 320 radio-frequency discharge ion source at energies from 1 to 2 keV and then accelerated across a single gap to the desired energy. The beam then passed through an einzel lens and steering magnet en route to a 30° magnetic ion-beam mass analyzer. This analyzer consisted of a c-yoke magnet possessing 10-cm circular pole pieces and a 3-cm gap. The beam then entered a 7-cm-long differentially pumped collision chamber that had entrance and exit apertures 0.16 cm in diameter. The differential pumping system employed two 4-in. diffusion pumps backed by mechanical pumps, a cryogenic refrigerator, and a liquid-nitrogen trap. From the collision chamber the beam passed into an observation chamber with a 25-cm-long glass window running parallel to the beam. After leaving the observation chamber the beam was collected in a Faraday cup. Elimination of secondary electron losses from the Faraday cup was achieved through the use of deep-cup geometry and a suppressor ring biased to -180 V. The Faraday-cup current was measured with a model 414A Keithley electrometer.

The radiation passing through the window of the

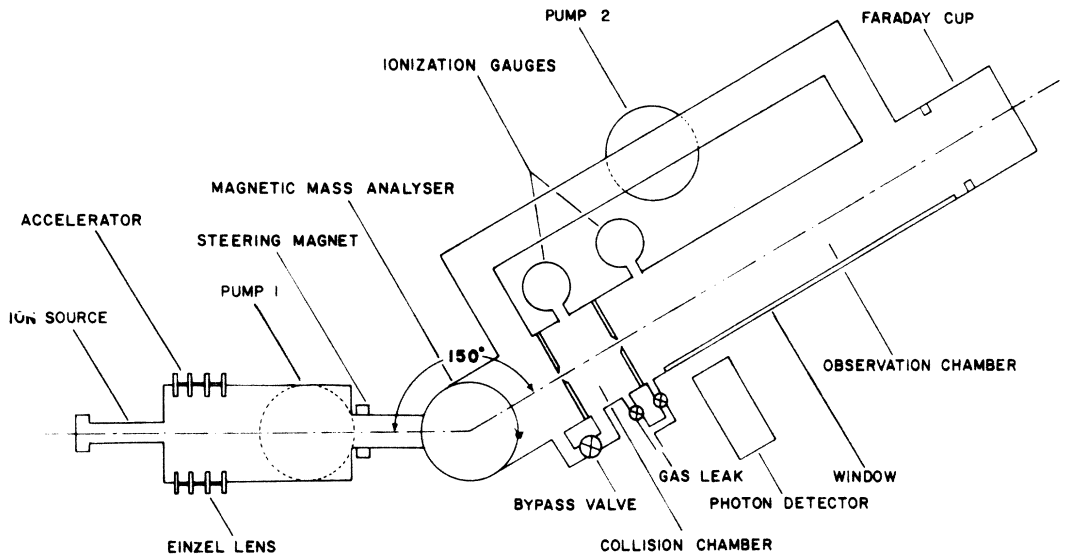

FIG. 1. Schematic diagram of the apparatus as viewed from above (not to scale). The entrance and exit apertures of the collision chamber define the angular acceptance of the beam.

observation chamber was detected by a photomultiplier tube mounted on a track parallel to the beam direction. A unit-magnified image of a 1-cm segment of the beam was projected onto the photocathode by a lens system. Baird-Atomic B-11 filters of the appropriate passband were used to eliminate all but the H_α or H_β radiation. Cooling of the photomultiplier to ice-water temperatures increased the ratio of signal to noise and stabilized the drift. The signal from the photomultiplier was amplified and then recorded on a chart recorder. The signal due to the desired transitions was obtained by recording the difference between the photomultiplier output with the beam on and with the beam off.

For the Thoneman radio-frequency discharge source most investigators[13] have found inherent energy spreads of approximately 100 eV. An investigation of the shape of the proton and deuteron mass peaks showed that the resolution of the magnetic mass analyzer was such that no improvement on the inherent energy spread was obtained. Cross-section data were taken with the analyzer set on the mass peak.

The existence of a plasma potential can lead to a mean ion energy from 50 to 400 eV higher than the extraction voltage.[14,15] In this experiment a 200-eV plasma potential was assumed with a resulting uncertainty in the beam energy of about 200 eV.

PROCEDURE

With the gas pressure in the collision chamber fixed, the radiation intensity per unit beam current was measured. Measurements were taken

TABLE I. Cross sections in units of 10^{-19} cm^2.

H^+ energy [a] (keV)	Argon		Helium		Krypton	
	3s	4s	3s	4s	3s	4s
1.2	17.5±2.1	3.29±0.66	0.82±0.05	0.147±0.006	28.3±1.2	3.13±0.79
1.7	20.3±1.2	4.22±0.42	0.87±0.07	0.159±0.013	28.8±2.4	3.78±0.48
2.2	23.3±1.4	5.28±0.65	1.07±0.06	0.191±0.012	27.6±2.1	4.32±0.22
2.7	22.9±0.7	5.98±0.48	1.31±0.09	0.225±0.016	27.7±0.9	4.48±0.31
3.2	24.5±0.7	6.33±0.53	1.30±0.07	0.245±0.021	29.5±0.8	4.57±0.68
4.2	30.5±1.7	7.43±0.50	1.48±0.08	0.315±0.018	35.0±0.9	5.31±0.34
5.2	36.8±0.9	8.71±0.36	1.80±0.05	0.411±0.014	37.1±0.8	7.46±0.25
6.2	37.6±1.2	10.0±0.22	2.05±0.11	0.515±0.017	39.1±0.6	8.50±0.48
7.2	38.3±1.0	10.9±0.50	2.32±0.01	0.617±0.037	45.0±0.7	9.87±0.49
8.2	39.9±3.5	12.0±0.54	2.75±0.14	0.743±0.065	51.2±1.9	11.5±0.86

[a] Deuteron data listed at proton energy having same particle velocity as deuteron energy used.

at a distance from the collision-chamber-exit aperture greater than $\frac{2}{3} v\tau_{ns}$, where v is the velocity of the proton and τ_{ns} is the lifetime of the ns state. Since the radiative lifetimes of the $3s$, $3d$, and $3p$ states are 16.0×10^{-8}, 1.56×10^{-8}, and 0.54×10^{-8} sec, respectively, essentially all H_α radiation measured at distances beyond $\frac{2}{3} v\tau_{3s}$ is due to transitions from the $3s$ state.[1] The radiative lifetime of the $4s$ state, 23.0×10^{-8} sec, is sufficiently longer than the 2.6×10^{-8} sec radiative lifetime of the mixed state which includes the other H_β transitions to ensure adequate discrimination against those states at distances greater than $\frac{2}{3} v\tau_{4s}$.[2]

Gas pressures inside the collision chamber were such that beam attenuation varied between 6 and 13%. For beam attenuations in this range only single collision events should occur, with negligible scattering out of the beam. As a check on this some measurements were taken with a 3.5-cm-length target chamber. The results using the 3.5-cm chamber were in excellent agreement with the 7-cm-chamber data indicating no appreciable scattering out of the beam.

The proton (or deuteron) flux measured at the Faraday cup was corrected for attenuation due to neutralization inside the collision and observation chambers, and the mean flux in the collision chamber was used in the cross-section determinations.

Although the ratio of the pressure in the collision chamber to the pressure in the observation chamber was between 50 to 70 for all the runs, there was some H_α and H_β radiation produced by charge transfer from the gas outside the collision chamber. In order to correct for this, background radiation was measured in the following manner. The collision chamber was opened to the low-pressure region of the apparatus through a 1-in.-diameter valve, and the target gas was diverted into the observation chamber at a point near the collision-chamber-exit aperture. Gas flow was then adjusted until the pressure in the observation chamber was the same as that during the data run. Measurements of radiation intensity were made in the same manner as for a data run, and corrections were made to the data-run measurements.

Using protons as incident particles, measurements were made at accelerating potentials between 3 and 8 keV in 1-keV steps. With deuterons as incident particles, data were taken at accelerating potentials having particle velocities equivalent to proton accelerating potentials of 1, 1.5, 2, 2.5, 3, and 4 keV. A data run consisted of measuring the intensity per unit beam current 4 to 6 times at each energy of the above quoted ranges. The average of these 4 to 6 measurements was considered to represent the measured value for a given data run. When a data run was repeated, no attempts were made to adjust any changes in electronic gain. Instead repeated runs were normalized to the original run. The mean of all data runs taken (usually 3 to 5) is the quoted result. The error bars indicate the standard deviation from the mean.

Analysis of the data produced relative cross-section curves. Absolute values for the cross sections owing to impact on He and Ar were determined by normalizing the relative curves to the published values for absolute cross sections at 5 keV and

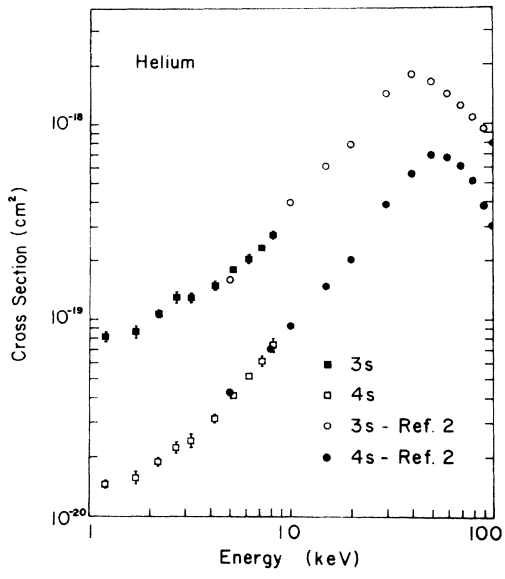

FIG. 2. Plot of $3s$ and $4s$ capture by H^+ and D^+ on He. Also shown are the data of Ref. 2.

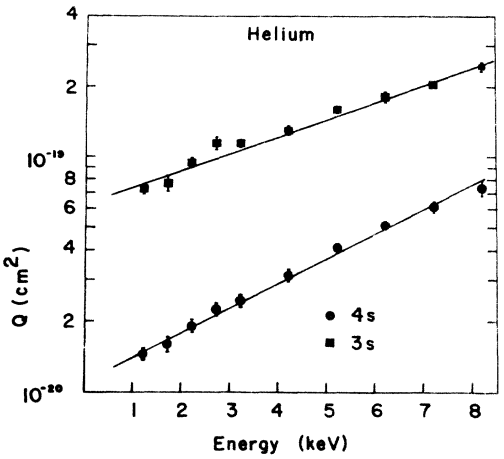

FIG. 3. Plot of $3s$ and $4s$ capture by H^+ and D^+ on He showing exponential increase in cross section with energy. A least-squares fit to the data was used to determine the slopes of the straight lines shown.

above.[1,2] Since an absolute value for the cross section owing to impact on Kr was not available, a different normalization procedure was needed. Absolute determination of the Kr cross sections required absolute-pressure measurements and calibration of the detection system. Absolute pressure was determined by measuring the beam attenuation of a 5-keV proton beam in Kr, and using the published value of the cross section for total charge exchange.[16] Calibration of the detection system was accomplished by taking the cross section for 4s and 3s capture owing to 5-keV proton impact on Ar as a known absolute value and measuring the appropriate cross section before each Kr data run.

RESULTS AND DISCUSSION

Graphs of the data tabulated in Table I are shown in Figs. 2–5. Energy values on these graphs represent the energy due to the equivalent proton accelerating potentials plus the energy due to the assumed 0.2-kV plasma potential. As previously noted, the error bars show the standard deviation from the mean of several trials and represent the reproducibility which typically varied between 5 and 15%. Factors restricting the reproducibility were poor signal-to-noise ratio, fluctuations in target-gas pressure and beam current, and short-term electronic drift.

Figure 2 shows log-log plots of the 3s and 4s capture cross section versus energy for proton and deuteron impact on He. Also shown are the measurements of Hughes *et al.*[2] which had previously found a maximum in the 3s cross section at 40 keV and maximum in the 4s cross section at 50 keV. No evidence for any additional structure is seen in the present results.

Figure 3 shows a plot of the logarithm of the He cross section versus a linear energy scale for the energy range of the present experiment. The straight lines drawn through the data represent a least-squares fit to the function $e^{E/K}$, where K = 6.0 keV for 3s and K = 4.2 keV for 4s.

Figure 4 shows log-log plots of the 3s and 4s capture cross section versus energy for proton and deuteron impact on Ar. Also shown are the measurements of Hughes *et al.*[2] The present data seem to confirm the secondary maximum in the 3s cross section near 6 keV previously reported. There is evidence of additional structure near 2 keV in the 3s cross section.

This experiment shows no evidence for any structure in the 4s cross section for protons on Ar below 10 keV.

Figure 5 shows log-log plots of the 3s and 4s capture cross section versus energy for proton and deuteron impact on Kr. No other measurements have been made of these cross sections for this target.

The flat region below 3 keV may indicate some structure in the 3s cross section. The fact that the magnitude of the cross section changes so little over the entire range measured makes it less clear that the behavior below 3 keV is indeed indicative of structure.

The 4s cross section varies fairly smoothly with energy. There may be some indication of change in slope between 3 and 4 keV.

ACKNOWLEDGMENTS

We wish to thank Tim Heumier, Kelly Knowlton, and Barbara Nibling for their able assistance in taking the data.

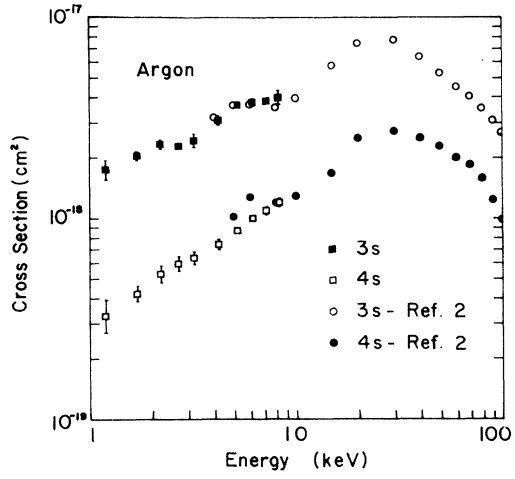

FIG. 4. Plot of 3s and 4s capture by H^+ and D^+ on Ar. Also shown are the data of Ref. 2.

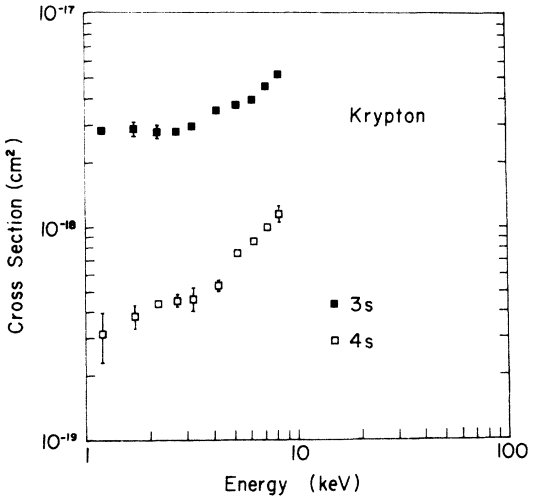

FIG. 5. Plot of 3s and 4s capture by H^+ and D^+ on Kr.

†This research was supported by the Robert A. Welch Foundation.

[1]R. H. Hughes, H. R. Dawson, B. M. Doughty, D. B. Kay, and C. A. Stigers, Phys. Rev. 146, 53 (1966).
[2]R. H. Hughes, H. R. Dawson, and B. M. Doughty, Phys. Rev. 164, 166 (1967).
[3]J. R. Oppenheimer, Phys. Rev. 31, 349 (1928).
[4]J. D. Jackson and H. Shiff, Phys. Rev. 89, 359 (1953).
[5]D. R. Bates and A. Dalgarno, Proc. Phys. Soc. Lond. A66, 972 (1953).
[6]D. Rapp and W. E. Francis, J. Chem. Phys. 37, 2631 (1962).
[7]H. S. W. Massey, Rep. Prog. Phys. 12, 248 (1949).
[8]H. S. W. Massey and E. H. S. Burhop, *Electronic and Ionic Impact Phenomena* (Clarendon, Oxford, England, 1952), pp. 513 and 514.
[9]S. Dworetsky, R. Novick, W. W. Smith, and N. Tolk, Phys. Rev. Lett. 18, 939 (1967).
[10]R. A. Mapleton, Phys. Rev. 122, 528 (1961).
[11]D. Jaecks, B. Van Zyl, and R. Geballe, Phys. Rev. 137, A340 (1965).
[12]J. B. Hasted and J. B. H. Stedeford, Proc. R. Soc. Lond. A277, 466 (1955).
[13]M. D. Gabovich, *Plasma Ion Sources* (Naukova Dumka, Kiev, 1964) [English transl.: By U. S. Air Force Systems Command (Wright Patterson Air Force Base, Ohio) (unpublished)].
[14]C. J. Cook, O. Heinz, D. C. Lorentz, and J. R. Peterson, Rev. Sci. Instrum. 33, 649 (1962).
[15]D. Blanc and A. Degeilh, J. Phys. Radium 22, 230 (1961).
[16]S. K. Allison, Rev. Mod. Phys. 30, 1137 (1958).